Phase Diagram and High-Pressure Boundary of Hydrate Formation in the Carbon Dioxide-Water System

ARTICLE *in* THE JOURNAL OF PHYSICAL CHEMISTRY B · JUNE 2009

Impact Factor: 3.3 · DOI: 10.1021/jp9008493 · Source: PubMed

THE JOURNAL OF PHYSICAL CHEMISTRY B

Article

Phase Diagram and High-Pressure Boundary of Hydrate Formation in the Carbon Dioxide#Water System

Andrej Yu. Manakov, Yuriy A. Dyadin, Andrey G. Ogienko, Alexander V. Kurnosov, Eugeny Ya. Aladko, Eduard G. Larionov, Fridrih V. Zhurko, Vladimir I. Voronin, Ivan F. Berger, Sergei V. Goryainov, Anna Yu. Lihacheva, and Aleksei I. Ancharov

J. Phys. Chem. B, **2009**, 113 (20), 7257-7262• Publication Date (Web): 30 April 2009

Phase Diagram and High-Pressure Boundary of Hydrate Formation in the Carbon Dioxide−Water System

Andrej Yu. Manakov,*[,†,‡] Yuriy A. Dyadin,[§] Andrey G. Ogienko,[†,‡] Alexander V. Kurnosov,[†] Eugeny Ya. Aladko,[†] Eduard G. Larionov,[†] Fridrih V. Zhurko,[†] Vladimir I. Voronin,[||] Ivan F. Berger,[⊥] Sergei V. Goryainov,[#] Anna Yu. Lihacheva,[#] and Aleksei I. Ancharov[‡,▽]

Nikolaev Institute of Inorganic Chemistry SB RAS, Akademii. Lavrentiev Avenue, 3, Novosibirsk, 630090, Russian Federation, Novosibirsk State University, Pirogova Street 2, Novosibirsk, 630090, Russian Federation, Institute of Metal Physics UrB RAS, S. Kovalevskoj Street 18, Ekaterinburg, 620219, Russian Federation, Institute of Solid State Chemistry UrB RAS, Pervomajskaya Street 91, Ekaterinburg, GSP-145, 620041, Russian Federation, Institute of Geology and Mineralogy SB RAS, Academy Koptug Avenue, 3, Novosibirsk, 630090, Russian Federation, and Institute of Solid State Chemistry SB RAS, Kutateladze 18, Novosibirsk, 630128, Russian Federation

Received: January 29, 2009; Revised Manuscript Received: March 3, 2009

Experimental investigation of the phase diagram of the system carbon dioxide−water at pressures up to 2.7 GPa has been carried out in order to explain earlier controversial results on the decomposition curves of the hydrates formed in this system. According to X-ray diffraction data, solid and/or liquid phases of water and CO_2 coexist in the system at room temperature within the pressure range from 0.8 to 2.6 GPa; no clathrate hydrates are observed. The results of neutron diffraction experiments involving the samples with different CO_2/H_2O molar ratios, and the data on the phase diagram of the system carbon dioxide−water show that CO_2 hydrate of cubic structure I is the only clathrate phase present in this system under studied $P-T$ conditions. We suppose that in the cubic structure I hydrate of CO_2 multiple occupation of the large hydrate cavities with CO_2 molecules takes place. At pressure of about 0.8 GPa this hydrate decomposes into components indicating the presence of the upper pressure boundary of the existence of clathrate hydrates in the system.

Introduction

Clathrate hydrates are crystalline inclusion compounds in which the host framework is formed by hydrogen-bonded water molecules.[1] The cavities of the framework are occupied by the guest molecules of appropriate size and molecular shape. The host−guest interaction in true clathrate hydrates is exclusively of van der Waals nature. The hydrates formed by guest components existing as gas under normal conditions are conventionally termed gas hydrates. As a rule, gas hydrates existing at moderate pressures (less than 100 MPa) belong to one of three structural types: cubic structure I (CS-I), cubic structure II (CS-II), or hexagonal structure III (HS-III or sH). Various aspects of structural and physical chemistry of low-pressure gas hydrates were discussed in refs 1 and 2. Because low pressures can induce only minor variation of lengths of the hydrogen bonds and angles between them, only few structural types of gas hydrates are realized, while at high pressures the water framework is adjusted to the size and shape of the guest molecules, thus achieving the highest possible complementarity between the guest molecules and the cavities of the structure, as well maximizing overall density.

Structures of high-pressure clathrate hydrates of different substances such as methane, argon, and tetrahydrofuran, etc., and phase diagrams of the corresponding systems were reported in refs 3−13. At low pressures the CS-I hydrate is formed in the system CO_2-H_2O,[14,15] the decomposition curve of this hydrate was determined up to the pressure of tens of MPa (the data were summarized in refs 1, 14, and 15). The results reported in refs 14 and 16 show that the degree of filling of small cavities with CO_2 molecules rapidly increases with pressure and becomes larger than 0.8 at about 10 MPa. At 20 MPa, almost 100% occupation of small cavities occurs.[17] The CS-I hydrate is stable up to 500 MPa;[11] the existence of the CO_2 hydrates at higher pressure remained questionable. The results obtained at the first stage of the present study (reported in ref 18) essentially disagreed with the data available from the literature.[11,19] The controversy in experimental data can occur due to (a) formation of solid solutions of CO_2 in the CS-I framework, (b) formation of other hydrates with other concentration fields of existence in the system, and (c) high mutual solubility of carbon dioxide and water at pressure above 100 MPa. Therefore, the goal of the present work is to determine the possibility of formation of new high-pressure gas hydrates in the CO_2-H_2O system and the possibility of formation of carbon dioxide solid solutions in the clathrate framework of cubic structure I and to consider the probable $P-T-X$ phase diagram of this system in the $P-T$ region of hydrate formation. In the present work we pay special attention to the explanation of the discrepancies between our earlier experimental data[18] and the data presented in ref 11.

Experimental Section

The data for the carbon dioxide hydrate decomposition curve were obtained by differential thermal analysis (DTA) under high pressure of carbon dioxide, the technique being described in

* To whom correspondence should be addressed. Tel.: (7-383) 316 53 46. Fax: (7-383) 330 94 89. E-mail: manakov@che.nsk.su.
† Nikolaev Institute of Inorganic Chemistry SB RAS.
‡ Novosibirsk State University.
§ Deceased.
|| Institute of Metal Physics UrB RAS.
⊥ Institute of Solid State Chemistry UrB RAS.
Institute of Geology and Mineralogy SB RAS.
▽ Institute of Solid State Chemistry SB RAS.

10.1021/jp9008493 CCC: $40.75
Published on Web 04/30/2009

detail in ref 13. Samples of inert powder (SiC) wetted with 2−3 drops of distilled water were loaded into the DTA container having a volume of 0.05 mL. The samples were weighed before and after wetting in order to determine the amount of water. The container was hermetically attached to a stainless steel vessel supplied with a movable piston (a volume of 0.5−8 mL, depending on the position of the piston) and a check valve. After that, the vessel was pressurized with CO_2 gas up to the pressure of 2 MPa. The amount of CO_2 gas in the container was derived using the calculated volume of the container and the pressure of the gas; the estimated accuracy of this value is ±10−15%. The series of DTA experiments was performed with varying CO_2/H_2O molar ratio. The assembled cell was placed into a high-pressure hydrostatic chamber filled with a silicon oil−hexane mixture. The pressure was transmitted into the cell by the piston. Temperatures of phase transitions were registered as the moment of maximal difference in temperatures between the reference thermocouple and the thermocouple introduced into the sample container on quasiisobaric heating of the DTA cell. The duration of seasoning was varied from several minutes to 1−2 days. No significant trend in the hydrate decomposition temperatures was observed over this time scale. The appearance of peaks at the differential curve corresponding to heat absorption in the sample (hereafter thermal effects) evidenced occurrence of phase transitions. The maximum of the peak at the differential curve corresponds to the decomposition temperature of the gas hydrate. In typical experiments, the decomposition points of the CO_2 hydrates were measured with a chromel−alumel thermocouple (K-type) in the standard DTA scheme at a heating rate of 1−2 °C/min. The thermocouple was calibrated using reference points or a reference thermometer. The error in temperature measurement by the thermocouple did not exceed 0.2 °C. The pressure was measured with Bourdon pressure gauges (up to 250 MPa) calibrated using a load-piston manometer. At higher pressures, we used a manganine manometer calibrated against the melting point of mercury. Relative uncertainty of pressure measurements was about ±1% for pressures above 200 MPa (manganine manometer, maximum error 10 MPa at the pressure of 1 GPa) and ±0.5% for lower pressures (Bourdon pressure gauge, maximum error 1 MPa at the pressure of 200 MPa). The adequacy of our hardware and the experimental procedure was repeatedly proved by comparison of our experimental data to the data available from the literature (nitrogen−water system,[20] hydrogen−water system,[21] argon−water system,[22] methane−water system,[23] and ethane−water system [24]). In the course of our experiments the correctness of the measurements was periodically checked by registration of the high-pressure decomposition curve of the methane hydrate.

The sample of carbon dioxide hydrate for neutron diffraction experiments was synthesized at room temperature in a high-pressure piston−cylinder cell designed for in situ neutron diffraction measurements[25] from thoroughly ground D_2O ice and an excess of carbon dioxide under pressures of 250 (first experiment) and 210 MPa (second experiment). Both components were loaded in the cell at liquid nitrogen temperature. Neutron diffraction experiments were performed on a research reactor IVV-2 M (Ekaterinburg)[26] at $\lambda = 1.805$ Å. The X-ray diffraction study was performed using synchrotron radiation at the fourth beamline of the VEPP-3 storage ring (Siberian synchrotron and terahertz radiation center, Budker Institute of Nuclear Physics SB RAS), at $\lambda = 0.3675$ Å.[27] The Debye−Scherrer geometry was used. Diffraction patterns were collected using a MAR345 image plate detector (pixel size, 100 μm). Diffraction images were integrated with the FIT2D program;[28] the distance from the sample to the detector was determined using the diffraction patterns of a standard substance (NaCl). Deconvolution of peaks, search for possible indexing, refinement of unit cell parameters, and calculation of theoretical diffraction patterns were carried out with programs FullProf[29] and XLAT.[30] Raman spectra were recorded in situ in a diamond anvil cell at room temperature. We used a DILOR OMARS 89 spectrometer equipped with a Princeton Instruments LN/CCD1100PB CCD detector. The 514.5 nm line of an argon ion laser was used for excitation. The detector was calibrated using the characteristic lines of a neon lamp. The uncertainty in the position of spectral bands $\Delta\nu$ was ±1.0 cm^{-1}. A detailed description of the high-pressure diamond anvil cell is given in ref 31. Pressure in the cell was measured from the baric shift of the R_1 and R_2 lines of ruby fluorescence using the pressure calibration proposed in ref 32.

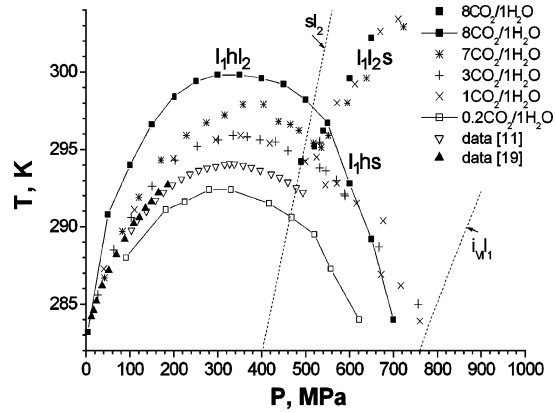

Figure 1. Experimental data on phase transformations in the CO_2−water system. Melting curves of solid CO_2 and ice VI are shown by solid lines marked sl_2 and $i_{VI}l_1$, respectively: i_{VI}, ice VI; l_1, water-rich liquid phase; l_2, CO_2-rich liquid phase; s, solid CO_2.

TABLE 1: Decomposition Temperatures of the CS-I Gas Hydrate of Carbon Dioxide at Different Pressures (h, CS-I Hydrate; l_1, Water-Rich Liquid Phase; l_2, CO_2-Rich Liquid Phase; s, Solid CO_2)

P, MPa	*T*, K	coexisting phases	*P*, MPa	*T*, K	coexisting phases
50	290.8	l_1hl_2	400	299.6	l_1hl_2
100	294.0	l_1hl_2	450	299.2	l_1hl_2
150	296.6	l_1hl_2	500	298.2	l_1hl_2
200	298.4	l_1hl_2	550	296.7	l_1hl_2
250	299.4	l_1hl_2	600	292.8	l_1hs
300	299.8	l_1hl_2	650	289.2	l_1hs
350	299.8	l_1hl_2	700	284.0	l_1hs

Results and Discussion

Experimental DTA data obtained for carbon dioxide−water mixtures with varying molar ratios are shown in Figure 1. The data obtained in refs 11 and 19 are shown for comparison. The numerical data corresponding to the highest temperature curve at the pressures below 0.8 GPa are shown in Table 1. One can see that an increase in the CO_2/H_2O molar ratio results in systematic shift of the experimental decomposition curve of the CO_2 hydrate to higher temperatures. In all cases the decomposition curves are smooth and have a characteristic bow-shaped outline. At low pressures all experimental curves are similar and reasonably agree with the low-pressure data reported[1,19] (Figure 1). The experimental data presented in ref 11 were obtained under an excess of water; hence, the CO_2/H_2O molar ratio in these experiments was lower than in our experiments.

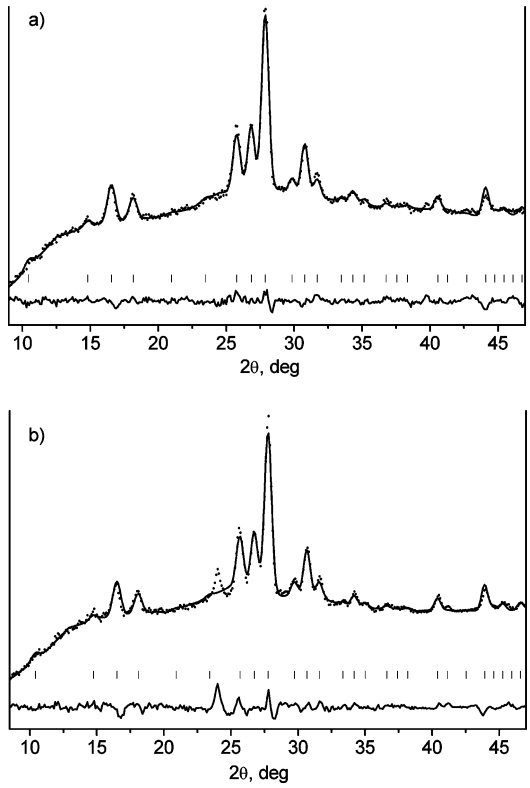

Figure 2. Powder diffraction patterns of the CO_2 hydrate. (a) P = 250 MPa, T = 273 K, and bulk composition of the sample is $CO_2 \cdot 1.2D_2O$; (b) P = 210 MPa, T = 273 K, and bulk composition of the sample is $CO_2 \cdot 6.3D_2O$. Experimental data and a simulated diffraction pattern are shown by dots and a solid line, respectively. Calculated positions of reflections are indicated by tick marks. The difference between the observed and calculated intensities is illustrated by the bottom solid line.

The corresponding decomposition curve is in good agreement with our data obtained at small CO_2/H_2O molar ratio (Figure 1). The decomposition curves cross the line of CO_2 melting in the pressure interval of 460−520 MPa; at higher pressures the experimental curves fork. We speculate that the hydrate decomposition curves observed at pressures below 460−520 MPa correspond to decomposition of the CO_2 hydrate (h) to aqueous phase (l_1) saturated with CO_2 and liquid CO_2 saturated with water (l_2). The highest of these curves corresponds to monovariant curve l_1hl_2, while others correspond to decomposition of the CO_2 hydrate with nonequilibrium composition (a less probable version that other curves correspond to divariant equilibria hl_1 or hl_2). This point and phase equilibria at higher pressures are discussed below.

We carried out neutron diffraction investigation of the mixtures of carbon dioxide and D_2O having two different compositions at the pressure range of 200−250 MPa and the temperature of 0 °C (Figure 2). It appeared that no hydrates of other structures are formed under the conditions of these experiments. Also, there was no direct evidence supporting the hypothesis of the possible formation of solid solutions of carbon dioxide in the CS-I hydrate. Powder neutron diffraction patterns of the hydrates prepared from the samples of different compositions (Figure 2) perfectly matched the model of the CS-I hydrate having all cavities filled (a = 11.895 ± 0.003 Å, V = 1683.1 ± 0.9 Å^3 at the pressure of 250 MPa and composition of the starting mixture of $CO_2 \cdot 1.16D_2O$; a = 11.926 ± 0.005 Å, V = 1694.4 ± 1,4 Å^3 at the pressure of 210 MPa and composition of the starting mixture of $CO_2 \cdot 6.3D_2O$). We believe that

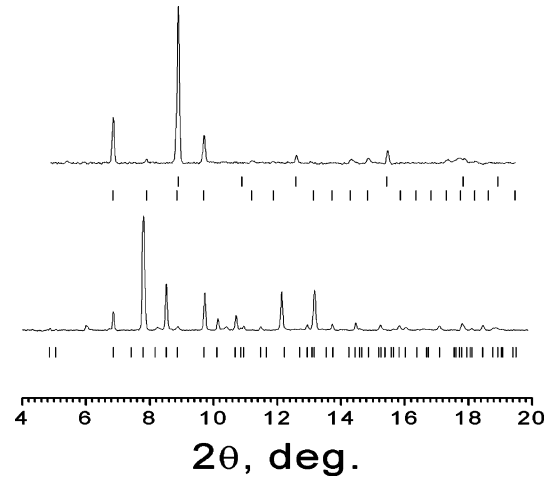

Figure 3. (Bottom) Powder diffraction pattern of the carbon dioxide−water mixture at 1.8 GPa and room temperature. Tick marks correspond to positions of reflections expected for ice VI with the unit cell parameters a = 6.138 Å and c = 5.682 Å. (Top) Powder diffraction pattern of the carbon dioxide−water mixture at 2.6 GPa and room temperature. Tick marks correspond to positions of reflections expected for ice VII with the unit cell parameter a = 3.352 Å (top marks) and solid carbon dioxide with the unit cell parameter a = 5.326 Å (bottom marks).

formation of clathrate hydrates outside the studied interval of CO_2/H_2O molar ratios is impossible. Refinement was carried out with the reflections starting from $2\theta = 15°$. The appearance of one extra reflection at $2\theta = 24°$ in the diffraction patterns taken at 210 MPa (Figure 2b) is most likely caused by diffraction of the primary beam on the thermostat hardware. In both cases the crystal structures were refined using the Rietveld procedure (Figure 2). The initial unit cell parameter, atomic positions, and site occupation factors were taken from ref 33. It turned out that this structural model fits the diffraction patterns after introducing only one modification: the degree of filling of the small cavities with carbon dioxide molecules was taken to be ∼1. After refinement of the unit cell parameter and the positions of the framework atoms (causing almost no changes in their coordinates), an excellent agreement between the calculated and experimental patterns was achieved. Attempts to alter the arrangement of molecules in the cavities did not lead to further improvement. It should be noted that accurate determination of occupancy of the hydrate cavities is not possible on the basis of our diffraction patterns. First of all, we have a low ratio of the number of measured reflections to the number of refined parameters. In addition, thermal parameters of the guest molecules and occupancy of the hydrate cavities show strong correlation: the occupation factors can be increased by decreasing thermal parameters of the guest molecules, and vice versa. Therefore, we found out that a single hydrate of the CS-I type with the composition close to $CO_2 \cdot 5.75D_2O$ is formed in the system at pressures below 550 MPa; precise determination of the composition of this hydrate from our data was not possible.

To determine the phase composition of the system in the pressure interval of 500−1100 MPa and above 1100 MPa, we obtained the diffraction patterns of the mixtures of carbon dioxide and water at pressures up to 2.6 GPa at room temperature. Under the pressures up to 2.2 GPa, the diffraction patterns contain reflections presumably corresponding to ice VI (Figure 3; two reflections at ∼6 and ∼12° most likely correspond to the ruby chips which were used as a pressure gauge). Unit cell parameters of ice VI calculated from our data are a = 6.14 Å and c = 5.68 Å at 1.8 GPa and room temperature

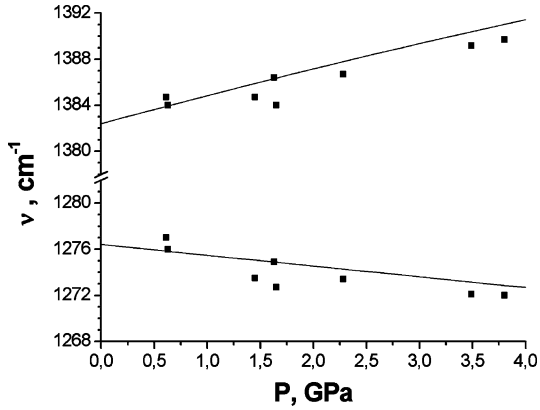

Figure 4. Pressure shift of Fermi-resonance Raman bands of solid CO_2 at high pressures and room temperature: points, our data; solid lines, data of ref 36.

(literature data for 1.1 GPa and 225 K: $a = 6.181$ Å, $c = 5.698$ Å [34]). The diffraction patterns recorded at the pressure of 2.6 GPa simultaneously exhibit the reflections of ice VII and solid carbon dioxide (Figure 3). Unit cell parameter of ice VII at 2.6 GPa and room temperature calculated from our data is $a = 3.35$ Å; the literature data $a = 3.344$ Å at 2.4 GPa.[34] The unit cell parameter of solid carbon dioxide is $a = 5.33$ Å at 2.6 GPa and room temperature; the literature data $a = 5.346$ Å under the same conditions[35] (Figure 3). We did not try to refine X-ray data with use of the Rietveld method because diffraction rings were spotty in all cases. Therefore, it was shown in the diffraction experiment that no unknown phases are formed at room temperature in the system carbon dioxide−water within the considered pressure range. This conclusion is also confirmed by the results of our Raman spectroscopy experiments in diamond anvil cells (Figure 4). A comparison of our spectra to the data reported in ref 36 shows that within the pressure range of 0.5−4.0 GPa (at room temperature) the spectra of the samples under investigation contain only the bands corresponding to the solid carbon dioxide phase. No peak shifts indicative of the formation of clathrate or nonclathrate hydrates of carbon dioxide were observed under these conditions. Finally, it was shown recently[37] (we became aware of this work after completion of our experiments) that the CS-I hydrate of carbon dioxide decomposes at the temperature of about 250 K and pressure of about 1.2 GPa, yielding ice VI, which is stable under these conditions, and solid carbon dioxide; therefore, the upper pressure boundary of the hydrate stability at this temperature was found; this is in good agreement with the spectroscopic and structural data considered above.

Examining three possible reasons of the differences in experimental data (Figure 1; the possible reasons are (a) the formation of solid solutions of CO_2 in the CS-I framework, (b) the formation of several hydrates differing in concentration fields of existence in the system, and (c) the high mutual solubility of carbon dioxide and water at pressures above 100 MPa), we supposed that reason a is the case. The data on the solubility of carbon dioxide in water under pressures up to 200 MPa are presented in ref 38. Analysis of these data shows that at pressures of 200−300 MPa and temperatures of 273−293 K the solubility of carbon dioxide in water can be estimated as 4 mol of CO_2/(1 kg of water) (0.07:1 CO_2/H_2O). This result provides the evidence of a substantial extension of the field of water-rich liquid l_1 along the concentration axis, but it is not sufficient to explain our experimental data. We did not observe formation of different hydrates in neutron diffraction experiments. In addition, in case b (formation of two different stoichiometric hydrates) two monovariant decomposition curves should occur in the phase diagram. This contradicts our experimental data (Figure 1). Under high-pressure conditions two ways of formation of CO_2 solid solutions in the CS-I framework are possible: (a) variable occupation of small cavities and (b) multiple occupation of large cavities by CO_2 molecules. The data presented in ref 17 show that CO_2 hydrates synthesized at pressures of about 20 MPa have hydrate numbers $n \leq 5.75$ ($CO_2 \cdot nH_2O$). It corresponds to at least 100% occupation of both types of the cavities in the CS-I framework; hence, existence of vacant small cavities at pressures of several hundred MPa looks improbable. We believe that multiple occupation of the large cavities by CO_2 molecules takes place in our case. The following indirect considerations support this hypothesis. The van der Waals volume of the CO_2 molecule is 34 Å^3.[39] The large cavity of the CS-I hydrate framework can accommodate guest molecules as large as sulfur hexafluoride[40] or tetrahydrofuran[41] with van der Waals volumes of 74 and 77 Å^3, respectively. Under the high-pressure conditions the decomposition temperature of the CO_2 CS-I hydrate is significantly lower in comparison to other CS-I hydrates studied (at 320 MPa: CO_2 hydrate, 300 K; CH_4 hydrate, 318 K;[23] C_2H_6 hydrate, 317 K [24]); hence, CO_2 hydrate has more loose packing of crystalline framework in comparison with CH_4 and C_2H_6 hydrates. At high pressures decomposition temperatures of gas hydrates are very sensitive to the packing density of the crystalline framework; for example, the filling of empty small cavities in the cubic structure II tetrahydrofuran hydrate with xenon results in 70° increase in decomposition temperature.[42] Analysis of the data given above shows that multiple (double) occupation of large cavities of the CS-I framework is the most probable reason of formation of the solid solutions.

Using experimental data obtained in the present work and the literature data, we modeled a $P-T$ projection of the diagram of the binary system carbon dioxide−water (Figure 5). The existence of polymorphous forms of ice within the investigated pressure range gives rise to nonvariant equilibria involving different ice modifications (quadrupole points Q_5, Q_6, Q_7, and Q_9). The monovariant line hl_1l_2 of decomposition of the hydrate, coming out of the quadrupole point Q_3,[1] after passing through the maximum goes down and crosses the curve of carbon dioxide melting, thus forming the quadrupole point Q_4. With further pressure rise, the monovariant curve hsl_1 which comes out of the quadrupole point Q_4 and corresponds to decomposition of the hydrate into solid carbon dioxide and water-rich liquid l_1 crosses the curve $i_{VI}hl_1$, thus giving the quadrupole point Q_8. With further pressure increase, the quadrupole point Q_9 is formed; this is the point where high-pressure ices i_{VII} and i_{VI}, solid carbon dioxide, and l_l liquid are in equilibrium. Therefore, at pressure above the position of the quadruple point Q_8, the hydrate-forming system under investigation becomes a regular eutectic system; the slope of the monovariant line $i_{VI}sh$ going out from the quadruple point Q_8 illustrates to the pressure dependence of the high-pressure boundary of hydrate existence in the system. This conclusion corresponds to our X-ray and Raman data, which indicate coexistence of ices and solid CO_2 at pressures above 500 MPa and room temperature. The appearance of the reflections of solid carbon dioxide in the diffraction patterns at 2.6 GPa can be caused only by the crossing of the monovariant curve $i_{VII}sl_1$, which corresponds to pressure-induced crystallization of carbon dioxide from its aqueous solution. The Clapeyron equation predicts that the slope for the hydrate decomposition curves $l_1hl_2-l_1hs-i_{VII}hs$ to the pressure axis will decrease in this sequence. It is caused by

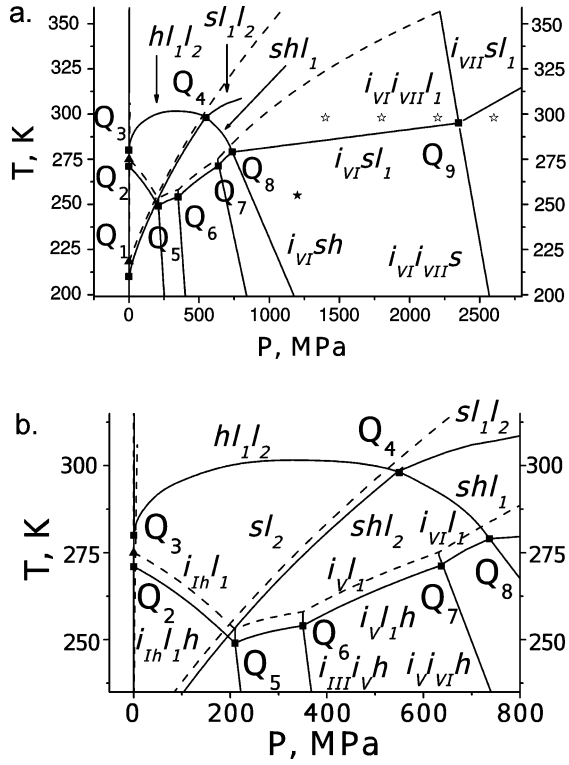

Figure 5. Pressure−temperature projection of the carbon dioxide−water system: h, CS-I hydrate of carbon dioxide; l_1, water-rich liquid phase; l_2, CO_2-rich liquid phase; s, solid CO_2; i_{Ih}, i_{III}, i_V, i_{VI}, and I_{VII}, ices Ih, III, V, VI, and VII, respectively; Q_1, quadruple point hl_2gs; Q_2, quadruple point $i_{Ih}l_1hg$; Q_3, quadruple point l_1hl_2g; Q4, quadruple point l_1hl_2s; Q_5, quadruple point $i_{III}i_{Ih}l_1h$; Q_6, quadruple point $i_Vi_{III}l_1h$; Q_7, quadruple point $i_{VI}i_Vl_1h$; Q_8, quadruple point $i_{VI}l_1hs$; Q_9, quadruple point $i_{VII}i_{VI}l_1s$. Details are omitted in the low-pressure part of the diagram. Triangles correspond to triple points in the respective single-component systems; two-phase equilibrium curves in these systems are denoted by dotted lines. Open stars correspond to pressures and temperatures at which X-ray diffraction experiments have been conducted in this work. The point at which decomposition of CS-I hydrate to components occurred in ref 37 is denoted by the solid star.

crystallization of liquid water and carbon dioxide phases. The curve $i_{VII}hs$ has the smallest negative slope to the pressure axis (Figure 5) and represents the highest expected decomposition pressures of the CS-I carbon dioxide hydrate. The pressure of hydrate decomposition exceeding the expected one experimentally observed in ref 37 (solid star in Figure 5) may originate from kinetic hindering of the decomposition process in the situation when the initial hydrate and the reaction products are solids, as it was discussed in refs 43 and 44. Concluding this section, we discuss two points concerning the formation of CO_2 solid solutions in the CS-I framework. $P-X$ cross-sections of the CO_2-H_2O phase diagram at pressures of 200 and 400 MPa are shown in Figure 6. Taking into account that double occupancy of the CS-I large cavities by CO_2 molecules results in composition of 0.3:1 CO_2/H_2O, one can see that under equilibrium conditions the CO_2 hydrate with the maximal CO_2 content should be formed in any CO_2-H_2O mixture richer in CO_2. We suppose that kinetic hindrance in formation of the CO_2 hydrate may result in the situation observed experimentally: under the conditions of our experiment formation of the equilibrium CO_2 hydrate with the maximal occupation of large T-cavities by CO_2 molecules is possible only at very high CO_2/H_2O molar ratios. We would like to underline that the presented interpretation of our data implies that only the highest curve obtained in our experiments corresponds to the real monovariant

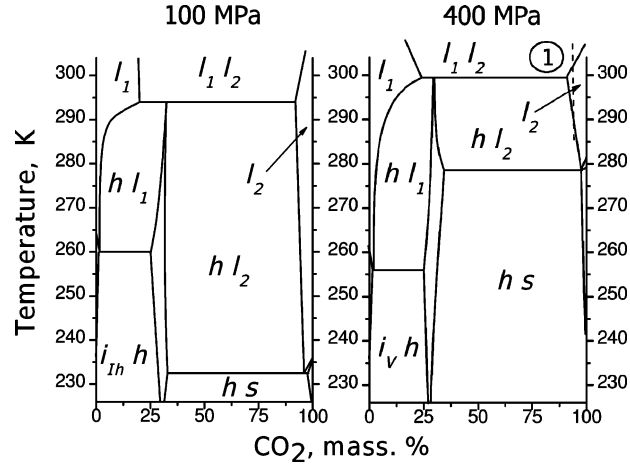

Figure 6. Temperature−composition cross-sections of the phase diagram of the CO_2-water system: h, CS-I hydrate of carbon dioxide; l_1, water-rich liquid phase; l_2, CO_2-rich liquid phase; s, solid CO_2. For other comments see the text.

equilibrium curve l_1hl_2. Other obtained curves correspond to nonequilibrium decomposition of CO_2 hydrate with a smaller content of CO_2. Further study is required to clarify features of the hydrate formation kinetics in this system. Another hypothetical possibility should be also discussed: the thermal effects observed in DTA experiments under the conditions of high CO_2/H_2O ratio correspond to separation of the l_2 phase into two liquid phases (respective line marked as "1" in Figure 6). In this case the formation of the monovariant curve l_1hs is not possible (Figures 1 and 5); hence, this hypothesis contradicts our experimental data.

It should be noted that there is a similarity of the system under study with the system sulfur dioxide−water investigated in detail in ref 45 at pressures up to 400 MPa. In both systems, the CS-I hydrates exist; the curves of their decomposition pass through a temperature maximum at a pressure about 300 MPa (330 MPa for CO_2 and 307 MPa for SO_2). It is noteworthy that at low pressure the decomposition temperature of the SO_2 hydrate is higher than that of the carbon dioxide hydrate, while at high pressures the situation is inverted. Most likely, this is due to substantially higher solubility of SO_2 in water and rapid increase in this value with pressure rise. Indeed, at 210 MPa the hydrate of sulfur dioxide begins to melt congruently; i.e., its content in water becomes higher than that in the hydrate. Such a situation is not achieved for carbon dioxide within the pressure range of hydrate existence.

In our experiments we have demonstrated that three atomic linear molecules are not capable of formation of ice-like high-pressure hydrates. In addition to carbon dioxide, a similar situation in hydrate formation may be expected for carbon disulfide, acetonitrile, etc. The frameworks with the cavities of the corresponding shape are not formed; this means that this observation puts additional restriction on the set of possible hydrate frameworks.

Acknowledgment. This work was supported by the Integration project No. 43 SB RAS and the Presidium RAS Program P-9-3 "Investigations of the matter at extreme conditions". A.G.O. and A.I.A. thank CRDF (Projects Y5-C-08-09 and Y5-C-08-01) and the project of Russian ministry of education (Projects RNP2.2.2.3.16035 and RNP2.2.2.3.16033) for financial support.

References and Notes

(1) Sloan, E. D.; Koh, C. A. *Clathrate Hydrates of Natural Gases*, 3nd ed.; CRC Press, Taylor and Francis Group: Boca Raton, FL, 2008.

(2) Jeffrey, G. A. Hydrate inclusion compounds. In *Comprehensive Supramolecular Chemistry*; Atwood, J. L., Davies, J. E. D., MacNicol, D. D., Vogtle, F. , Eds.; Elsevier Science: Oxford, U.K., 1996; Vol. 6 (Solid-State Supramolecular Chemistry: Crystal Engineering), p 757.

(3) Loveday, J. S.; Nelmes, R. N.; Guthire, M. *Phys. Rev. Lett.* **2001**, *87*, 215501.

(4) Loveday, J. S.; Nelmes, R. J.; Guthrie, M.; Klug, D. D.; Tse, J. S.; Handa, Y. P. *Nature* **2001**, *410*, 661.

(5) Dyadin, Yu. A. ; Bondaryuk, I. V. ; Zhurko, F. V. Clathrate hydrates at high pressures. In *Inclusion Compounds*; Atwood, J. L., Davies, J. E. D., MacNicol, D. D. , Eds.; Oxford University Press: Oxford, U.K., 1991; Vol. 5 (Inclusion and Physical Aspects on Inclusion), p 213.

(6) Manakov, A. Y.; Voronin, V. I.; Kurnosov, A. V.; Teplych, A. E.; Komarov, V. Y.; Dyadin, Y. A. *J. Inclusion Phenom.* **2004**, *48*, 11.

(7) Kurnosov, A. V.; Komarov, V. Y.; Voronin, V. I.; Teplych, A. E.; Manakov, A. Y. *Angew. Chem., Int. Ed.* **2004**, *43*, 2922.

(8) Manakov, A. Yu.; Goryainov, S. V.; Kurnosov, A. V.; Likhacheva, A. Yu.; Dyadin, Yu. A.; Larionov, E. G. *J. Phys. Chem. B* **2003**, *107*, 7861.

(9) Hirai, H.; Uchihara, Y.; Fujihisa, H.; Sakashita, M.; Katoh, E.; Aoki, K.; Nagashima, K.; Yamamoto, Y.; Yagi, T. *J. Chem. Phys.* **2001**, *115*, 7066.

(10) Mao, W. L.; Mao, H.-K. *Proc. Natl. Acad. Sci. U.S.A.* **2004**, *101*, 708.

(11) Nakano, S.; Moritoki, M.; Ohgaki, K. *J. Chem. Eng. Data* **1998**, *43*, 807.

(12) Nakano, S.; Moritoki, M.; Ohgaki, K. *J. Chem. Eng. Data* **1998**, *44*, 254.

(13) Dyadin, Yu. A.; Larionov, E. G.; Mirinskij, D. S.; Mikina, T. V.; Aladko, E. Ya.; Starostina, L. I. *J. Inclusion Phenom.* **1997**, *28*, 271.

(14) Circone, S.; et al. *J. Phys. Chem. B* **2003**, *107*, 5529.

(15) Uchida, T. *Waste Manage.* **1997**, *17* (5,6), 343.

(16) Klapproth, A.; Goreshnik, E.; Staykova, D.; Klein, H.; Kuhs, W. F. *Can. J. Phys.* **2003**, *81*, 503.

(17) Circone, S.; Stern, L. A.; Kirby, S. H.; Durham, W. B.; Chakoumakos, B. C.; Rawn, C. J.; Rondinone, A. J.; Ishii, Y. *J. Phys. Chem. B* **2003**, *107*, 5529.

(18) Dyadin, Yu. A.; Larionov, E. G.; Manakov, A. Yu. *Proc. 4th Int. Conf. Gas Hydrates (Yokohama, May 19−23)* **2002**, 590.

(19) Takenouchi, S.; Kennedy, G. C. *J. Geol.* **1965**, *73*, 383.

(20) Dyadin, Yu. A.; Larionov, E. G.; Aladko, E. Ya.; Zhurko, F. V. *Dokl. Phys. Chem* **2001**, *378* (4−6), 159.

(21) Dyadin, Yu. A.; Larionov, E. G.; Zhurko, F. V.; Aladko, E. Ya.; Mikina, T. V.; Komarov, V. Yu. *Mendeleev Commun.* **1999**, 209.

(22) Dyadin, Yu. A.; Larionov, E. G.; Mirinski, D. S.; Mikina, T. V.; Starostina, L. I. *Mendeleev Commun.* **1997**, 32.

(23) Dyadin, Yu. A.; Aladko, E. Ya.; Larionov, E. G. *Mendeleev Commun.* **1997**, 34.

(24) Kurnosov, A. V.; Ogienko, A. G.; Goryainov, S. V.; Larionov, E. G.; Manakov, A. Yu.; Lihacheva, A. Yu.; Aladko, E. Ya.; Zhurko, F. V.; Voronin, V. I.; Berger, I. F.; Ancharov, A. I. *J. Phys. Chem. B* **2006**, *110*, 21788.

(25) Ivanov, D. F.; Litvin, B. N.; Savenko, L. S.; Smirnov, V. I.; Voronin, A. E.; Teplykh, A. E. *High Pressure Res.* **1995**, *14*, 209.

(26) Aksenov, V. I. *Prepr., Jt. Inst. Nucl. Res., Dubna, USSR* **1994**, D3-94-364.

(27) Ancharov, A. I.; Manakov, A.Yu.; Mezentsev, N. A.; Tolochko, B. P.; Sheromov, M. A.; Tsukanov, V. M. *Nucl. Instrum. Methods Phys. Res., Sect. A* **2001**, *470*, 80.

(28) Hammersley, A. P. *Fit2D Programm*; European Synchrotron Research Facility: 1987−2003.

(29) Rodriguez-Carvajal, J. *Abstracts of the Satellite Meeting on Powder Diffraction of the XV Congress of the IUCr*, Toulouse, France; 1990; p 127 (up-to-date information on the software may be found on the website http://www.ccp14.ac.uk/ccp/web-mirrors/fullprof).

(30) Rupp, B. *Scr. Metall.* **1988**, *22*, 1.

(31) Goryainov, S. V.; Belitsky, I. A. *Phys. Chem. Miner.* **1995**, *22*, 443.

(32) Munro, R. G.; Piermarini, G. J.; Block, S.; Holzapfel, W. B. *J. Appl. Phys.* **1985**, *57* (2), 165.

(33) Udachin, K. A.; Ratcliffe, C. I.; Ripmeester, J. A. *J. Phys. Chem. B* **2001**, *105*, 4200.

(34) Kuhs, W. F.; Finney, J. L.; Vettier, C.; Bliss, D. V. *J. Chem. Phys.* **1984**, *81* (8), 3612.

(35) Olinger, B. *J. Chem. Phys.* **1982**, *77*, 6255.

(36) Hanson, R. C.; Jones, L. H. *J. Chem. Phys.* **1981**, *75*, 1102.

(37) Loveday, J.; Maynard, H.; Nelmes, R.; Bull, C.; Guthrie, M. *Proc. 11th Int. Conf. Phys. Chem. Ice (Bremerhaven, Germany. June 23−28)* **2006**, 141.

(38) Duan, Z.; Sun, R. *Chem. Geol.* **2003**, *193*, 257.

(39) Webster, C. E.; Drago, R. S.; Zerner, M. C. *J. Am. Chem. Soc.* **1998**, *120*, 5509.

(40) Aladko, E. Ya.; Anchrov, A. I.; Goryanov, S. V.; Kurnosov, A. V.; Larionov, E. G.; Lihacheva, A. Yu.; Manakov, A. Yu.; Potemkin, V. A.; Sheromov, M. A.; Teplykh, A. E.; Voronin, V. I.; Zhurko, F. V. *J. Phys. Chem. B* **2006**, *110*, 21371.

(41) Zakrzewski, M.; Klug, D. D.; Ripmeester, J. A. *J. Inclusion Phenom.* **1994**, *17*, 237.

(42) Larionov, E. G.; Manakov, A. Yu; Zhurko, F. V.; Dyadin, Yu. A. *Russ. J. Struct. Chem.* **2000**, *41* (3), 476.

(43) Manakov, A. Yu; Goryainov, S. V.; Kurnosov, A. V.; Likhacheva, A. Yu; Dyadin, Yu. A.; Larionov, E. G. *J. Phys. Chem. B* **2003**, *107*, 7861.

(44) Kurnosov, A.; Dubrovinsky, L.; Kuznetsov, A.; Dmitriev, V. *Z. Naturforsch.* **2006**, *61b*, 1573.

(45) Berkum, J. G.; Diepen, G. A. M. *J. Chem. Thermodyn.* **1979**, *11*, 317.

JP9008493